

Intensity Correlations for Stars

Robin Kaiser

Institut de Physique de Nice
CNRS / Université de la Côte d'Azur



Intensity Correlation team in Nice



R.K.



W. Guerin



M. Hugbart



G. Labeyrie



S. Tolila

+ former postdocs and PhD :
A. Siciak
A. Dussaux
N. Matthews

Lagrange



F. Vakili



J.P. Rivet



O. Lai



C. Courde



J. Chabé



+ E. S. G. de Almeida
(Valparaíso, Chile)

+ M. Borges
(Rio de Janeiro, Brazil)



+ D. Rätzel (Bremen, Germany)

+ C. Pfeiffer (Bremen, Germany)



Outline

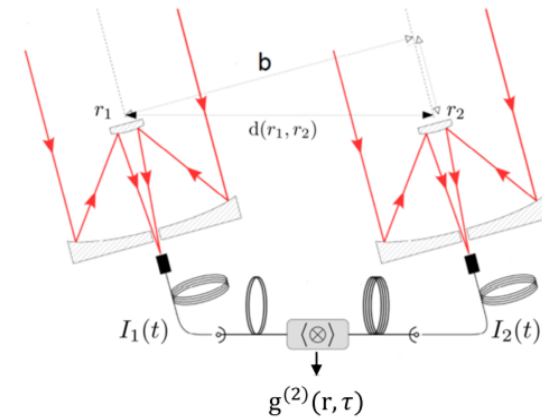
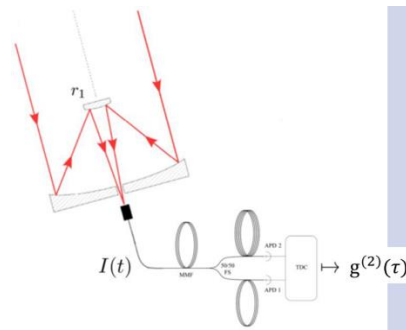
IC4Star project :

- 1) High angular resolution : white dwarf Sirius B**
- 2) Quantum optics from space : random lasing from Eta Car**

Second generation of intensity correlations for astrophysics

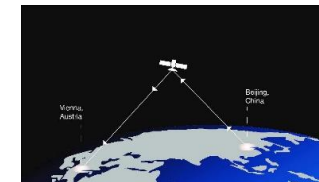
Goal : revive intensity correlation to

- Overcome baseline limitations by amplitude interferometry : $g^{(2)}(\mathbf{r})$
- Open an quantum optics eye to space observations : $g^{(2)}(\tau)$



Why now :

- Take advantage of quantum optics detection toolbox (fast photon counting)
- Record full temporal correlation function
- Combined expertise (astrophysics, atomic and quantum physics) available in Nice
- Maturing astrophysical community (CTA: Veritas / Magic, Asiago, ...)
- **Quantum Optics in Space for (quantum) communications**



Outline

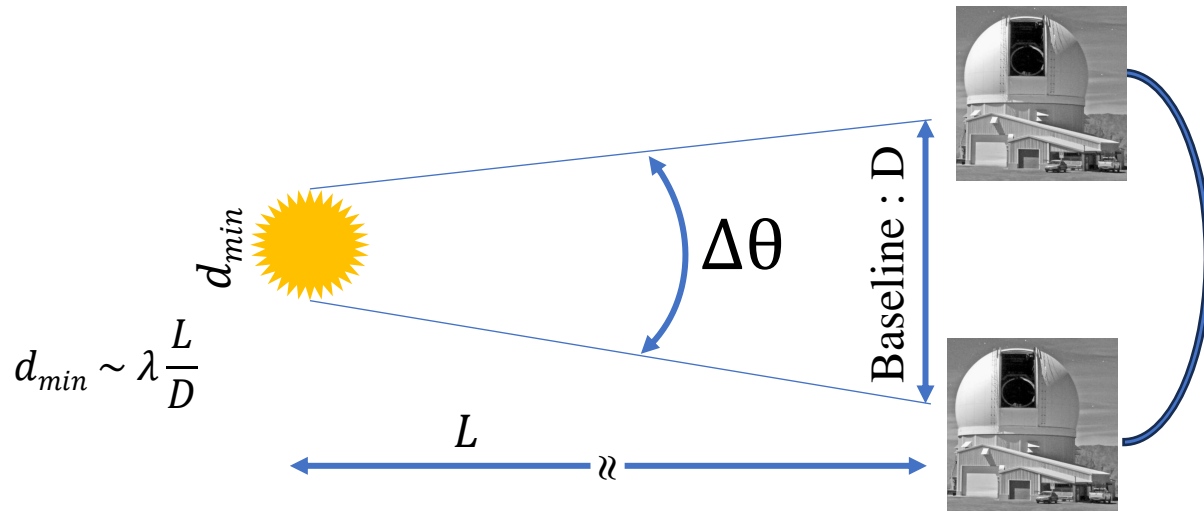
IC4Star project :

- 1) **High angular resolution : white dwarf Sirius B**
- 2) **Quantum optics from space : random lasing from Eta Car**

What next : IC4Stars



High angular resolution for stars : $\Delta\theta \sim \frac{\lambda}{D}$

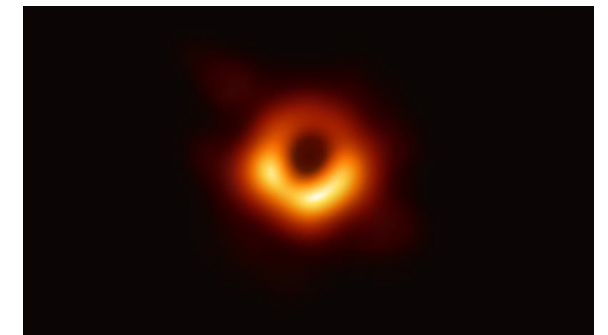


- i. interferometric recombination
(VLTI, Chara, NPOI < 300m)
- ii. **intensity correlations $g^2(\mathbf{r})$**
Hanbury Brown & Twiss

- 👍 Resilient to atmospheric turbulence (+ no adaptative optics required)
- 👍 Scalable to larger distances (ELT/VLT and beyond)
- 👍 Use of existing infrastructure
- 👍 **μ'' resolution** : similar to Event Horizon Telescope

$\lambda \sim 420\text{nm}, D \sim \text{km}$

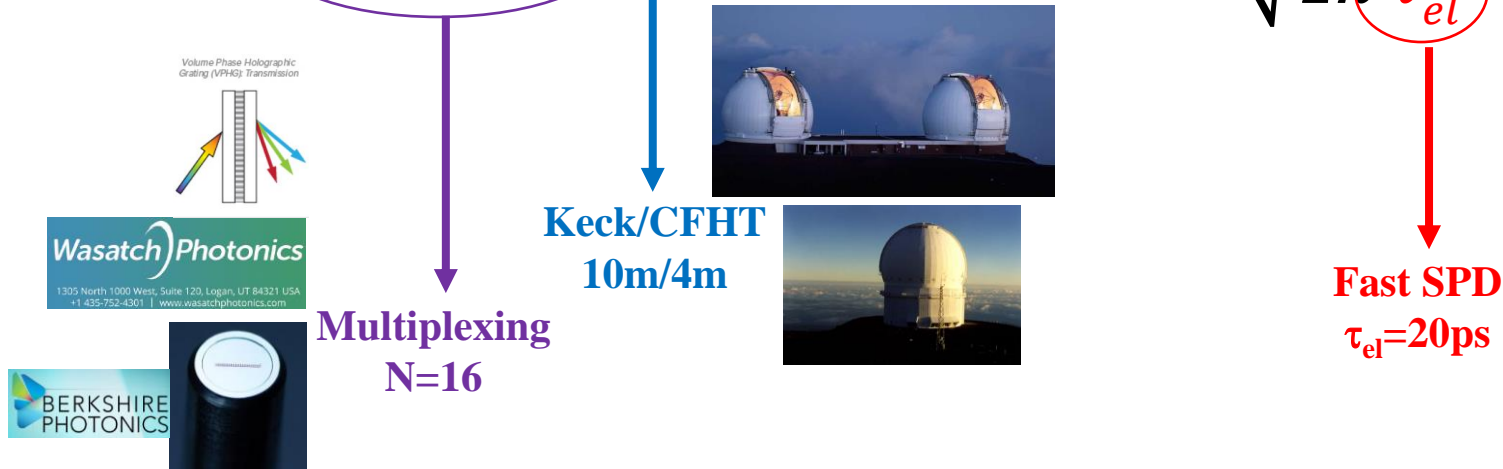
$\lambda \sim \text{mm}$
 $D = 12000 \text{ km}$



- The price to pay : low signal to noise ratio



$$SNR = \sqrt{N_{channel}} A \eta F(\nu) |V(r)|^2 \sqrt{\frac{T_{obs}}{2\pi \tau_{el}}}$$



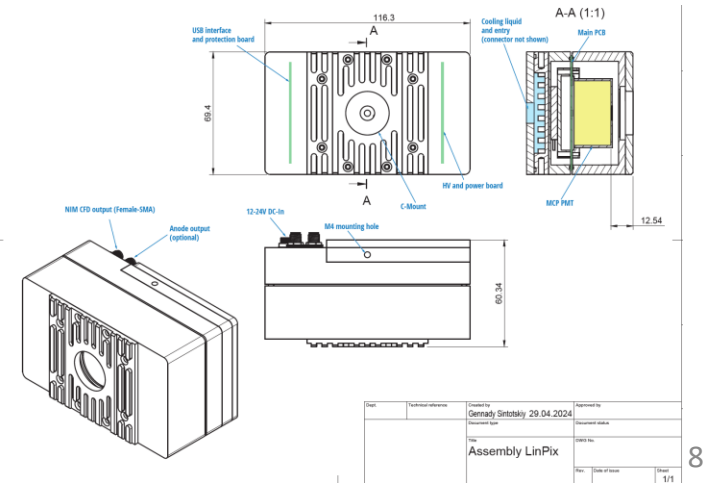
$$SNR : \quad \times 4 \quad \times 40 \quad \times 4 \Rightarrow \times 640$$

$T_{obs} \div 400\,000$

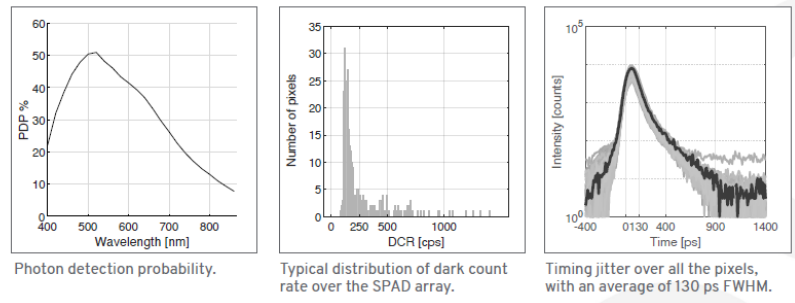
Photonscore : 2 x 16 LINPix



Max. recommended count rate, MHz	100
Shutdown count rate, MHz	110
Discrimination	Integrated CFD
Dark count rate, Hz	< 15 (Blue, Aqua), < 50 (Green), < 200 (Red)
Timing jitter, ps (FWHM)	< 35 (1MHz), < 45 (10MHz), < 75ps (100MHz)
Active area, mm	∅8
Dead time, ns	< 2



Pi Imaging : 2 SPADλ



pi imaging
ENABLING INNOVATION

SPADλ

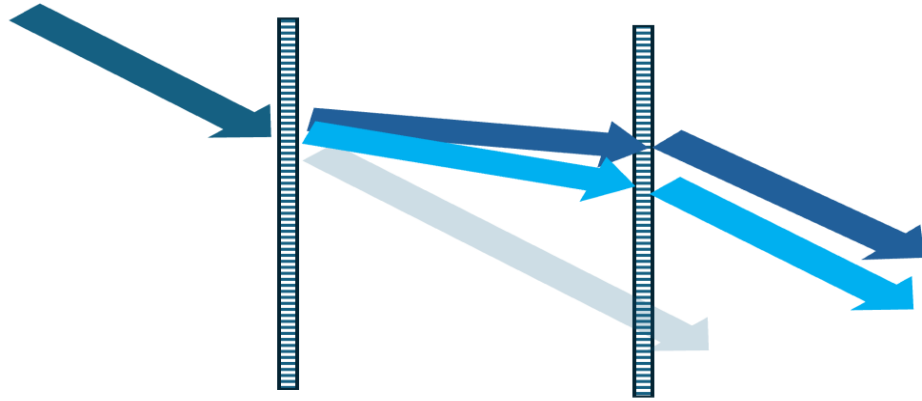
Description

SPADλ is a photon-counting linear array with time-gating and time-tagging. The core of the detector is a SPAD array with 320x1 pixels. Photon counting with up to 555'000 frames per second and zero readout noise is achieved. Nanosecond time gating is coupled with 17 ps gate phase shift. Time tagging with 20 ps resolution and 130 ps FWHM precision is available.

Typical technical specifications

SENSOR	LINEAR SPAD ARRAY
Image array	320 x 1
Pixel pitch	29 μm
Sensor wavelength range	400 to 900 nm
Peak photon detection probability	50% @ 520 nm
Fill factor with microlenses	>80 % for collimated light
Median dark count rate at room temperature	<250 cps
Percentage of pixels with >10 kcps	5%
Frame rate (max.)	555'000 fps
Dead time	10 ns
Timing jitter	130 ps FWHM
Time-tagging resolution	20 ps
Minimum exposure/gate width	2 ns
Minimum exposure/gate shift	17 ps
Crosstalk	2%
Connection type	C-mount

Multiplexing



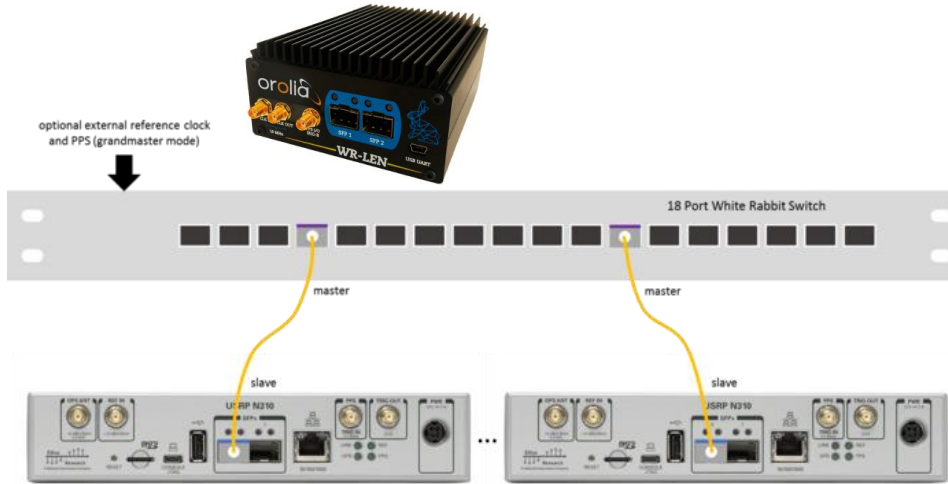
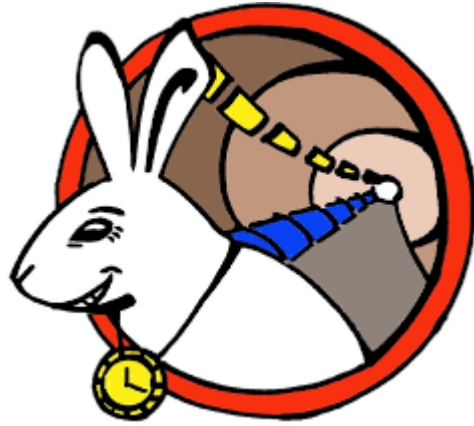
Dichroic:
420 : LINPix
500 : SPAD λ

To be done

- double system,
- efficiency
- calibration
- stability

Synchronisation @ ps over 1km

1)



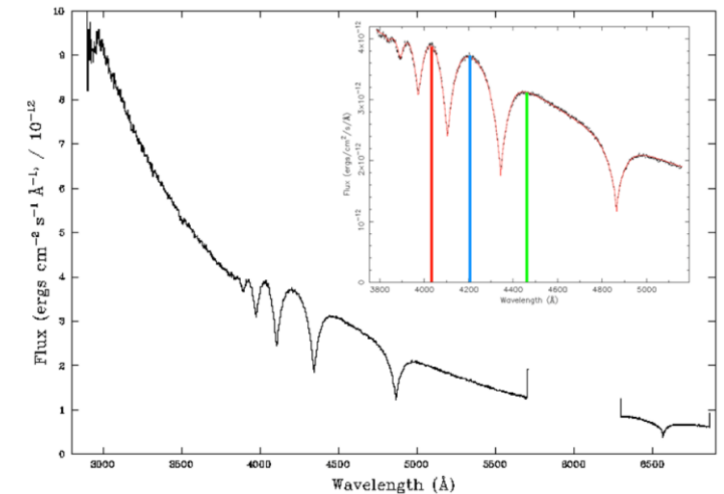
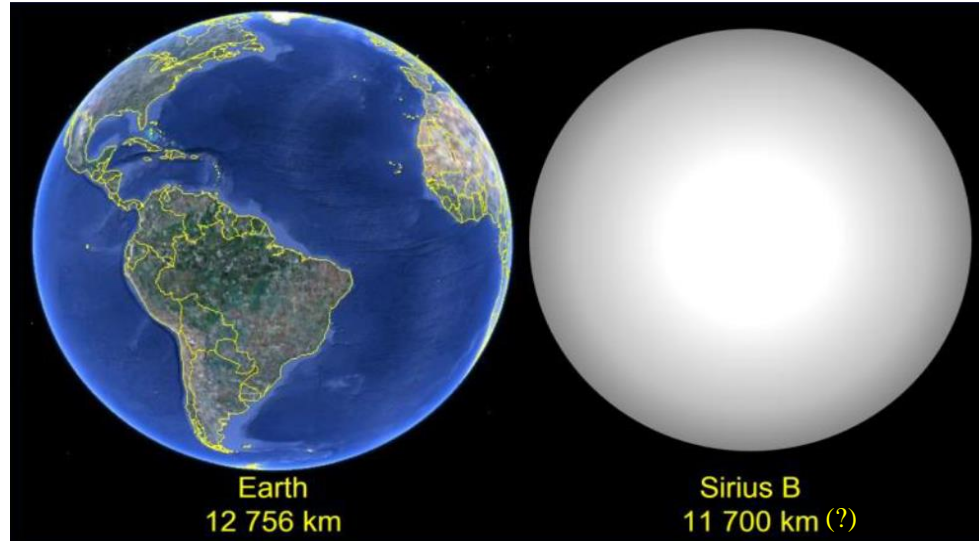
16 ps

2)

	Synchro White Rabbit Orolia COTS	Datation Swabian	Custom Sigmaworks Datation et Synchro
RMS timing PPS	< 40ps	42ps (100ps Test Géoazur)	< 1ps
RMS timing 10 MHz	15ps		< 1ps
Stabilité @ 1s	10ps	X	< 1ps
Stabilité @ long terme	20-45ps ?	X	<30fs
Cadence		70 Mhz	Min: 5 Mhz
Remarque			USB3
Canaux			2 x 16 canaux différentiel ou single ended
Coûts	~25k€ (5 switch)	80 k€ ?	~200k€
Développement	OTS	OTS	2 ans

1 ps

Angular resolution of a white dwarf



Count rates :

Sirius B

Quantum efficiency : 90%

Throughput : 20%

Keck: 110 000 cps

CHFT : 18 000 cps

D=11700km

L=8.6 light years= 8 10¹⁶m

$\Delta\theta=30\mu''$

The best direct test of stellar degeneracy is the determination of radii for white dwarfs in visual binaries (Table 1). In these cases, white dwarf masses are well determined from their orbital parameters, and stellar radii are derived from knowledge of effective temperatures and distances. Since



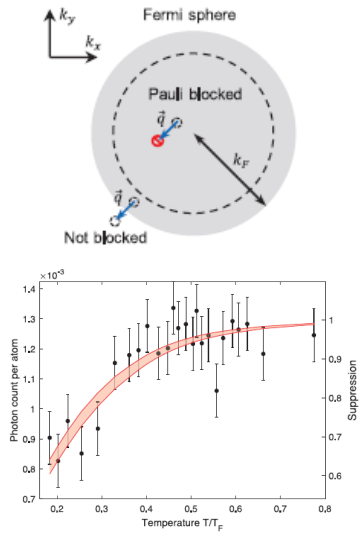
Pauli blocking for in degenerate Fermi gases

QUANTUM GASES

Pauli blocking of light scattering in degenerate fermions

Yair Margalit^{1,2*}, Yu-Kun Lu^{1,2}, Furkan Çağrı Top^{1,2}, Wolfgang Ketterle^{1,2}

Margalit *et al.*, *Science* **374**, 976–979 (2021)

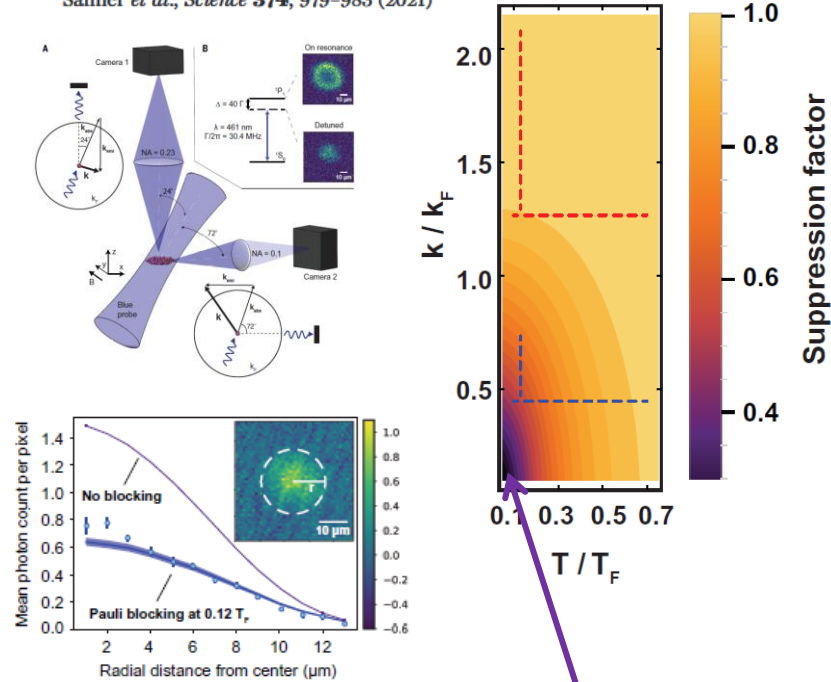


QUANTUM GASES

Pauli blocking of atom-light scattering

Christian Sanner^{*†}, Lindsay Sonderhouse[†], Ross B. Hutson, Lingfeng Yan, William R. Milner, Jun Ye^{*}

Sanner *et al.*, *Science* **374**, 979–983 (2021)



White dwarf :
 $T/T_f \sim 10^{-6}$
 $k/k_f \sim 10^{-6}$

nature communications

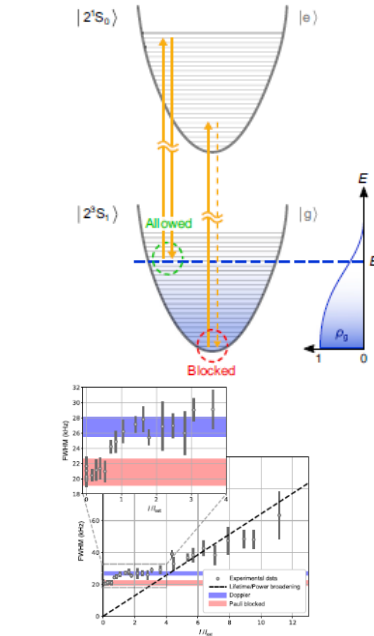


Article

<https://doi.org/10.1038/s41467-022-34135-6>

Pauli blocking of stimulated emission in a degenerate Fermi gas

Received: 24 March 2022 | Raphael Jamnin¹, Yuri van der Werf¹, Kees Steinhilber², Hendrick L. Bethlem^{1,2*} & Kjeld S. E. Eikema^{1,2*}

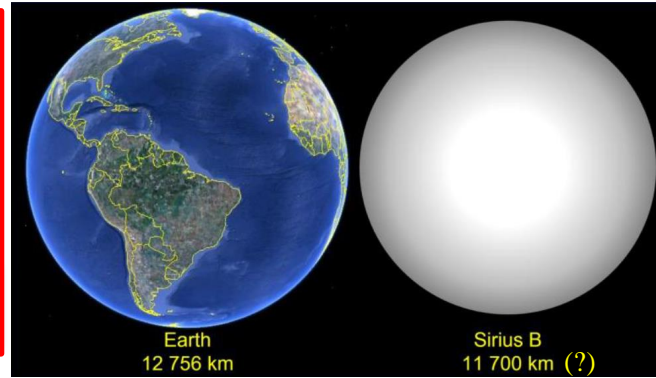


Light we see from Sirius B only from an outer shell of 100-300m

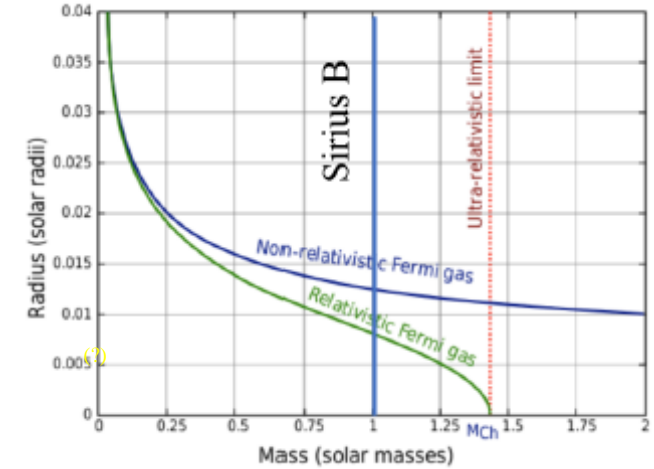
Path-opening on **Sirius B** (white dwarf) : quantum degenerate Fermi gas of electrons

SNR ≈ 6
in 1 hour
observation time !!!!

Beyond reach of present instruments



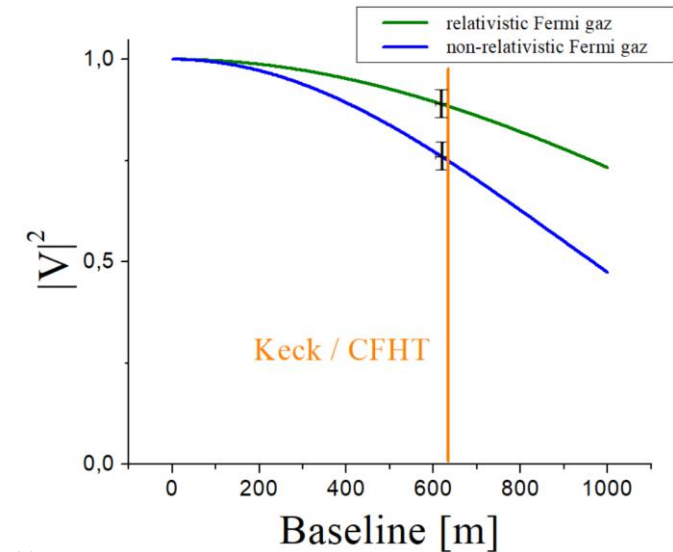
Magnitude=8.4



Mauna Kea @ Hawaii

Photon Bunching

- @ $\lambda = 420\text{nm}$
- $D=630\text{m}$



Sincerely,

John O'Meara
John O'Meara, Ph.D.
Chief Scientist and Deputy Director
jomeara@keck.hawaii.edu
+1 808 881-3855

Peter L. Wizinowich
Peter L. Wizinowich, Ph.D.
Chief of Technical Development
peterw@keck.hawaii.edu
+1 808 238 6648

Sincerely,

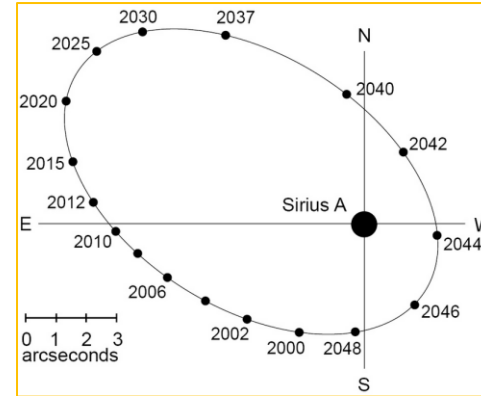
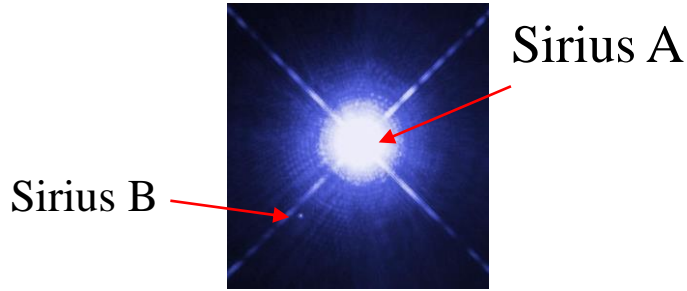
Jean-Gabriel Cuby
Jean-Gabriel Cuby
Executive Director
Canada-France-Hawaii Telescope

Mahalo,

Doug Simons
Doug Simons
Director
University of Hawaii's, Institute for Astronomy

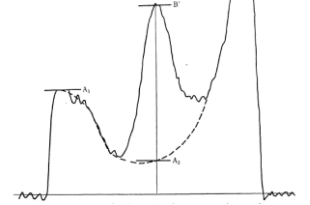
Background contribution of Sirius A

Sirius A / Sirius B : 10 000
@420nm : 1 000



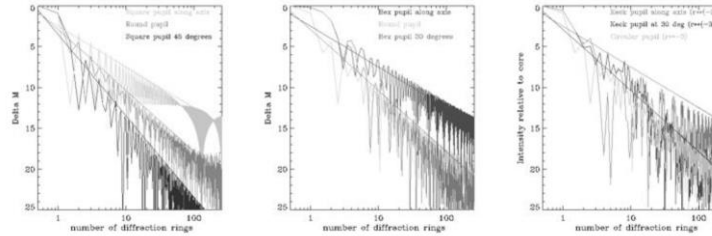
Okayama : Diameter 1.88m / Seeing: 1''
Equatorial mount

Nov, 27th 1966
Distance to Sirius A : 8''



- Turbulence** : does Adaptive Optics (AO) help?

- loss of flux and more complex logistics if we would do so
- beyond 5 arcsec AO is not helping, only corrects turbulence up to 2-4''
- At 10'' : diffraction more important than turbulence ($1/r^{11/3}$)



- Diffraction**

- Keck :**

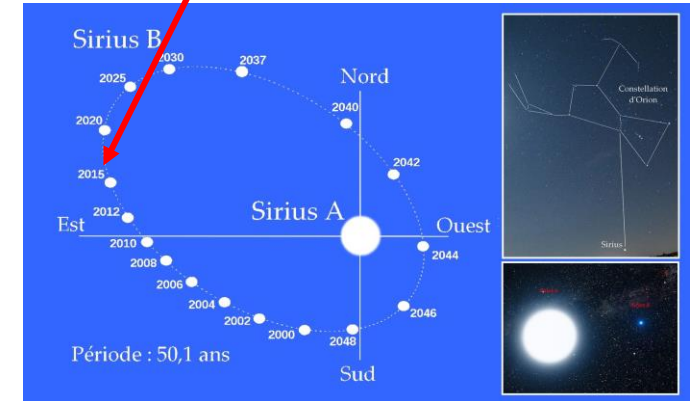
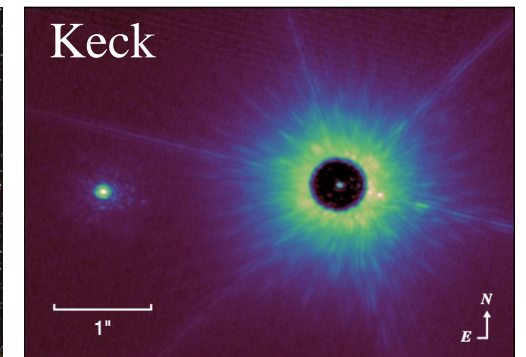
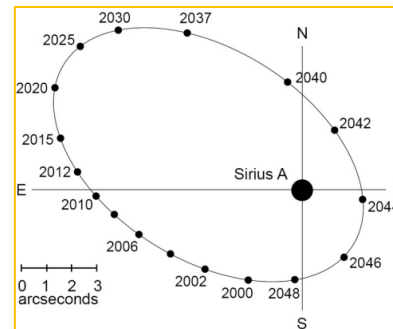
- segmented mirror : $1/r^2$ every 60 degrees of azimuth, $1/r^3$ at 30 degrees
- Alt-AZ mount : spiders ($1/r^2 - 1/r^4$) : rotate through image plane (loss of some data)

- CFHT :**

- Circular mirror : $1/r^3$
- Equatorial mount : 'fixed' spiders : $1/r^2$ - along north/south & east/west ; $1/r^4$ elsewhere : Sirius B 45° at north-west ☺

- Chopping :**

Dark count rate from Sirius B by tilting the detector out of Sirius B every 10s

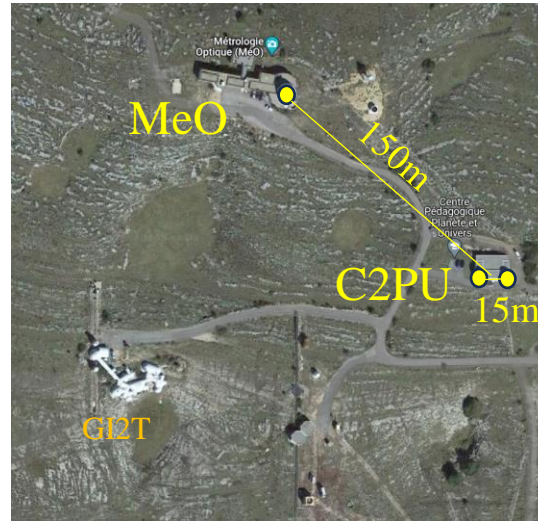


Benchmarking @ Calern

- WP2.1 : $g^2(r)$

yellow hypergiant : γ Cas : M4.5, 2.4 m''

O-type star : 10Lac : M4.88 0.11 m''



THE ASTROPHYSICAL JOURNAL, 869:37 (13pp), 2018 December 10
 © 2018. The American Astronomical Society. All rights reserved.

<https://doi.org/10.3847/1538-4357/aaec04>



Angular Sizes and Effective Temperatures of O-type Stars from Optical Interferometry with the CHARA Array

Kathryn D. Gordon¹, Douglas R. Gies¹, Gail H. Schaefer², Daniel Huber³, Michael Ireland⁴, and D. John Hillier⁵
¹Center for High Angular Resolution Astronomy and Department of Physics and Astronomy, Georgia State University, P. O. Box 5060, Atlanta, GA 30302-5060, USA; kgordon@astro.gsu.edu

²The CHARA Array of Georgia State University, Mount Wilson Observatory, Mount Wilson, CA 91023, USA

³Institute for Astronomy, University of Hawai'i, 2680 Woodlawn Drive, Honolulu, HI 96822, USA

⁴Research School of Astronomy & Astrophysics, Australian National University, Canberra, ACT 2611, Australia

⁵Department of Physics and Astronomy and Pittsburgh Particle Physics, Astrophysics, and Cosmology Center (PITT PACCC), University of Pittsburgh, Pittsburgh, PA 15260, USA

Received 2018 August 20; revised 2018 October 22; accepted 2018 October 22; published 2018 December 10

Identifier	Star Name	HD Number	Spectral Classification	V (mag)	B - V (mag)	V - K (mag)	T_{eff} (kK)	θ_{UD} (mas)
<i>a</i>	ζ Per	24912	O7.5 III(n)(f)	4.06	0.02	0.11	34.3 ± 0.8	0.216 ± 0.016
<i>b</i>	α Cam	30614	O9 Ia	4.29	0.05	0.05	29.4 ± 1.0	0.250 ± 0.014
<i>c</i>	λ Ori A	36861	O8 III(f)	3.47	0.01	-0.56	34.5 ± 0.8	0.219 ± 0.015
<i>d</i>	ζ Ori A	37742	O9.2 Ib	1.88	-0.11	-0.44	29.5 ± 1.0	0.546 ± 0.029
<i>e</i>	ζ Oph	149757	O9.2 IVnn	2.56	0.02	-0.06	32.1 ± 1.3	0.532 ± 0.010
<i>f</i>	10 Lac	214680	O9 V	4.88	-0.21	-0.62	35.5 ± 0.5	0.11 ± 0.02

Exciting targets for ultrahigh angular resolution in astrophysics :

- Wolf Rayet Stars
(before Supernovae type II explosion)



WR 124

M12 / 20 μ "

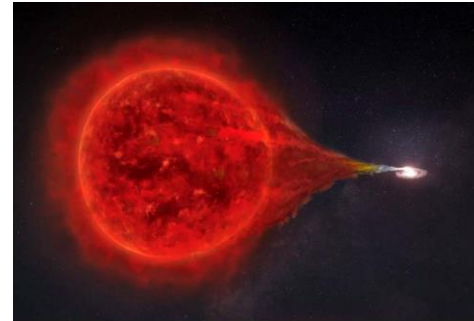
THE ASTROPHYSICAL JOURNAL SUPPLEMENT SERIES, 187:275-373, 2010 April
© 2010. The American Astronomical Society. All rights reserved. Printed in the U.S.A.

doi:10.1088/0067-0049/187/2/275

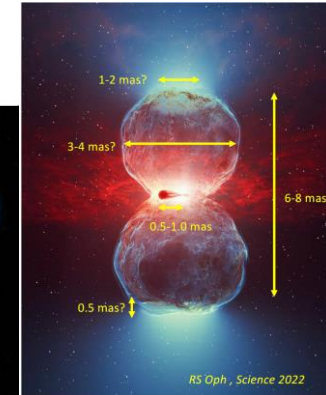
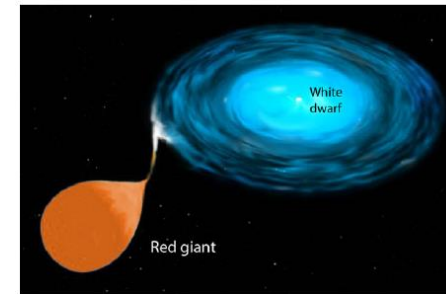
COMPREHENSIVE PHOTOMETRIC HISTORIES OF ALL KNOWN GALACTIC RECURRENT NOVAE

BRADLEY E. SCHAEFER
Physics and Astronomy, Louisiana State University, Baton Rouge, LA 70803, USA; schaefer@lsu.edu
Received 2009 April 6; accepted 2010 January 20; published 2010 March 17

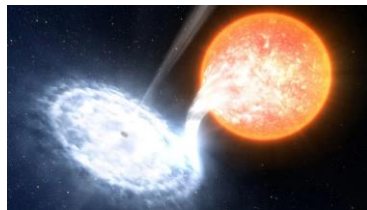
- Binary White Dwarfs
(before Supernovae type I explosion)



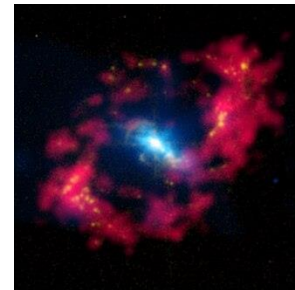
T Cor Bor: recurrent nova?
M10



- Black hole accretion disks

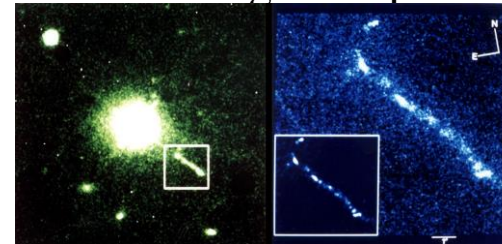


NGC4151



M11.5 / 100 μ "

3C 273 brightest quasar



(supermassive black hole)

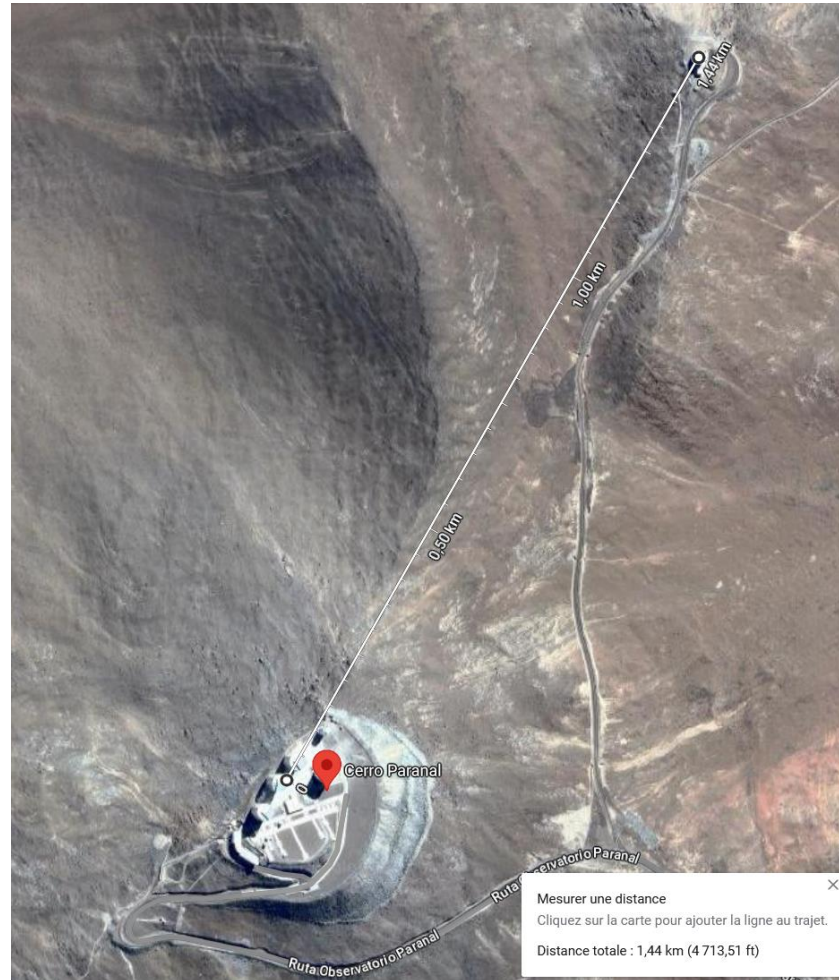
M12.9

0.55-0.9 mas

VLT + Vista : fibered instruments installed

4 UTs : 4*8.2m (effective 16.4m diameter) -> Espresso (380-780nm)

Vista 4m -> 4MOST (400-920nm)



Distance : 1.4km

Outline

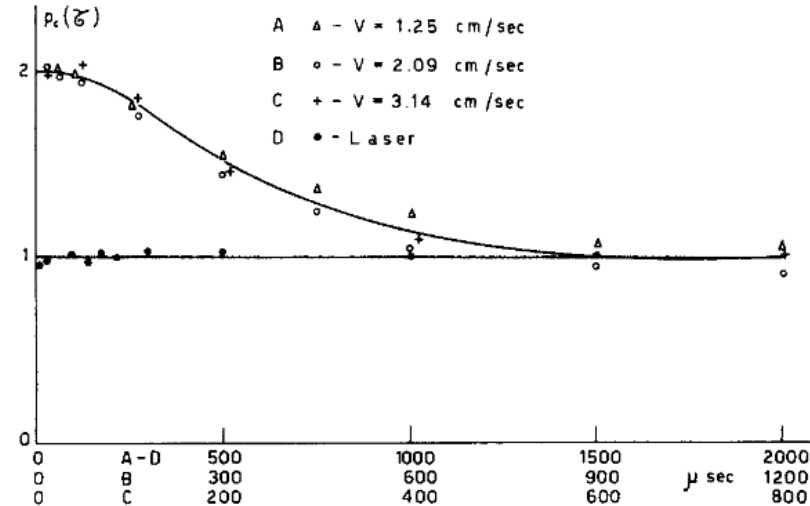
IC4Star project :

- 1) High angular resolution : white dwarf Sirius B
- 2) Quantum optics from space : random lasing from Eta Car

Second order coherence \neq first order coherence

Poisson statistics of laser $\Rightarrow g^{(2)}(\tau=0)=1$

Thermal light $\Rightarrow g^{(2)}(\tau=0)=2$



F.T. Arecchi, E. Gatti, A. Sona, Phys. Lett. 20, 27 (1966)

Quantum theory : R. Glauber (1963 \Rightarrow Nobel 2005)



g2 vs g1 : Second vs first order coherence

(i) $\langle E \rangle = 0$

(ii) Gaussian correlations

\Rightarrow Siegert relation:

$$g^2(\tau) - 1 \propto |g^1(\tau)|^2$$

Intensity correlations

TF [Optical spectrum $I(\omega)$]

Deviation from Siegert relation: lasing (⊕) or Non-Gaussian correlations (⊕)

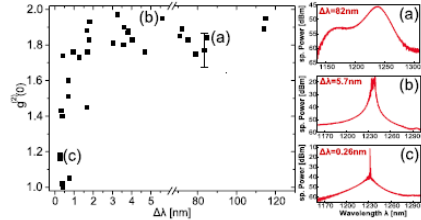
PHYSICAL REVIEW A 84, 063840 (2011)

Coherent and thermal light: Tunable hybrid states with second-order coherence without first-order coherence

Martin Blazek* and Wolfgang Eikelder†

Institute of Applied Physics, Technische Universität Darmstadt, Schlossgartenstrasse 7, D-64289 Darmstadt, Germany (Received 1 July 2011; published 19 December 2011)

We demonstrate the realization of a new hybrid state of light that is simultaneously spectrally broadband, i.e., incoherent in first order, and exhibits a laserlike normalized intensity correlation coefficient of 1.33, reflecting high coherence in second order. This is achieved by temperature-tuned light emission from an optoelectronic quantum dot superluminescent diode where the condensation of injected charge carriers into the globally lowest energy state of the strongly inhomogeneously broadened semiconductor quantum dot ensemble gives rise to a particular balance between spontaneous and stimulated emission.



VOLUME 86, NUMBER 20

PHYSICAL REVIEW LETTERS

14 MAY 2001

Photon Statistics of Random Lasers with Resonant Feedback

H. Cao, Y. Ling, J. Y. Xu, and C. Q. Cao

Department of Physics and Astronomy, Materials Research Center, Northwestern University, Evanston, Illinois 60208

Prem Kumar

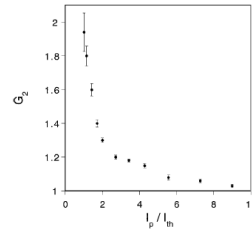


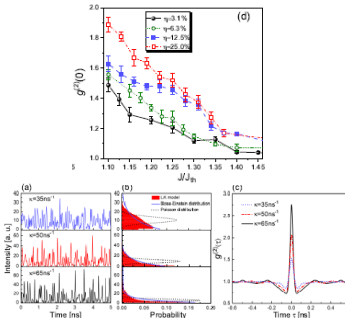
FIG. 4. The second-order correlation coefficient G_2 as a function of the ratio of the incident pump intensity I_p to the threshold intensity I_t .

Research Article
OPTICS EXPRESS

Vol. 26, No. 5 | 5 Mar 2018 | OPTICS EXPRESS 5991

Photon statistics and bunching of a chaotic semiconductor laser

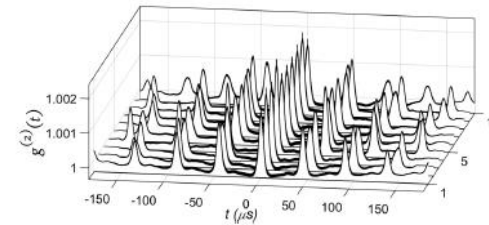
YANGIANG GUO,^{1,2} CHUNSHENG PENG,^{1,2} YULIN JI,^{1,2} PU LI,^{1,2} YUANYUAN GUO,^{1,2} AND XIAOMIN GUO^{1,2,*}



PHYSICAL REVIEW A 105, L031502 (2022)

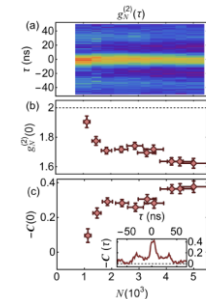
Intensity $g^{(2)}$ correlations in random fiber lasers: A random-matrix-theory approach

Ernesto P. Raposo,¹ Iván R. R. González,^{1,2} Edwin D. Coronel,² António M. S. Macêdo,¹ Leonardo de S. Menezes,^{4,5} Raman Kashyap,³ Anderson S. L. Gomes,³ and Robin Kaiser⁶



Non-Gaussian correlations in the steady-state of driven-dissipative clouds of two-level atoms

Giovanni Ferioli, Sara Pancaldi, Antoine Glienstein, David Clément, Antoine Browaeys,* and Igor Ferrier-Barbut†



$$g_N^{(2)}(\tau) = g_{\text{Gauss}}^{(2)}(\tau) + C(\tau)$$

arXiv:2311.13503v1

Statistics of Thermal and Laser Radiation

HENRI HODARA, SENIOR MEMBER, IEEE

Abstract—The random fluctuations of a signal constitute noise. Their magnitude which depends on the signal statistics may be significant in laser radiation. In this paper the statistics of thermal or incoherent radiation are briefly compared with those from an amplitude stabilized laser and the amplitude probability density of the uncoupled multimodal laser field is derived.

Proc. IEEE 53, 696 (1965)

Hodara formula :

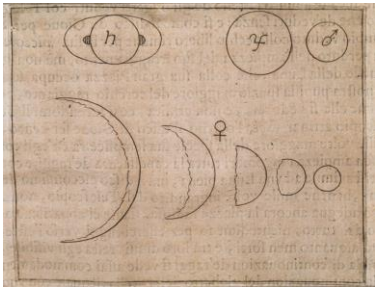
$$\text{RIN}_{\text{general}} = \frac{2e}{\langle i \rangle} + \frac{\langle i_{\text{sp}} \rangle^2}{\langle i \rangle^2} \cdot \frac{1}{\Delta\nu} = \frac{2e}{\langle i \rangle} + \frac{\beta^2}{\Delta\nu}$$

$\beta=1 \Leftrightarrow$ Siegert relation

$\beta=0 \Leftrightarrow$ laser

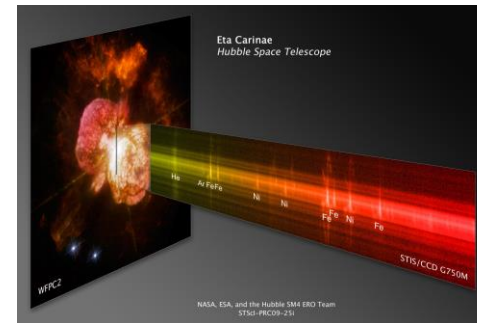
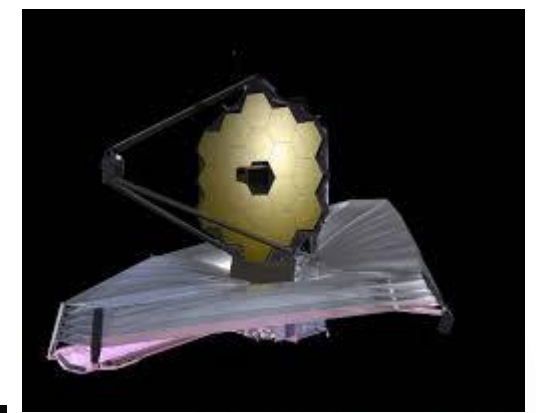
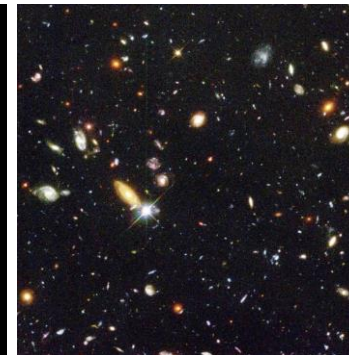
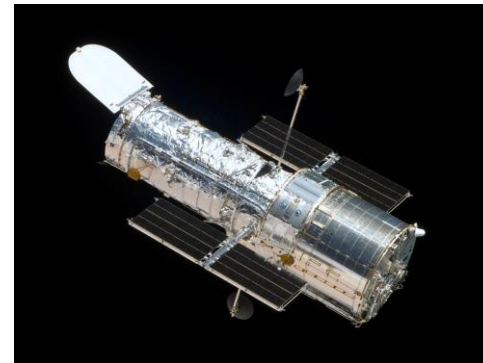
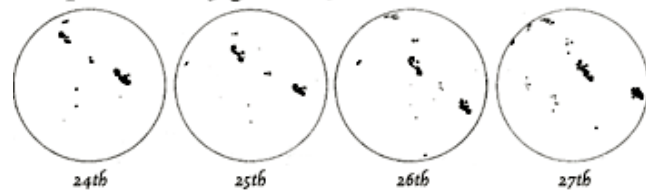
From Galileo (1564-1642) to Hubble Telescope (1990-2026?) & JWST

Direct imaging : large telescopes

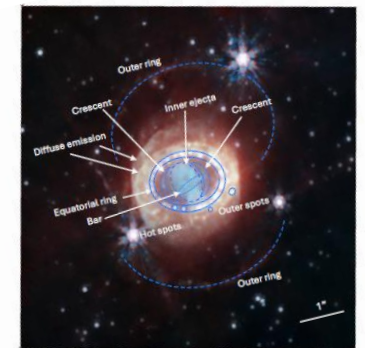


Phases of Venus

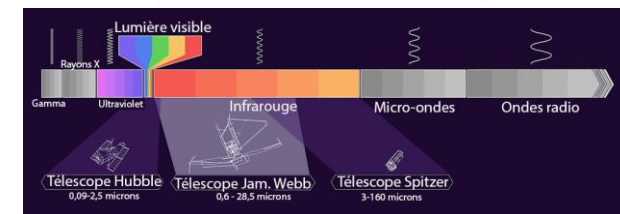
Sunspots drawn by Galileo, June 1612



Eta Carinae

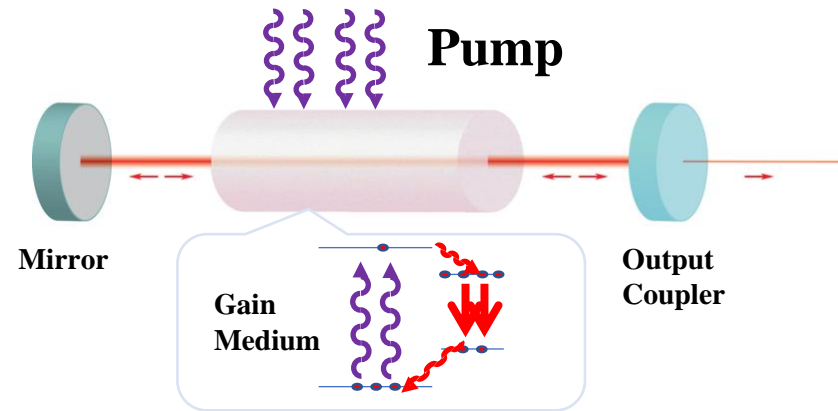


Black holes, dark matter,
universe expansion...



Random lasing

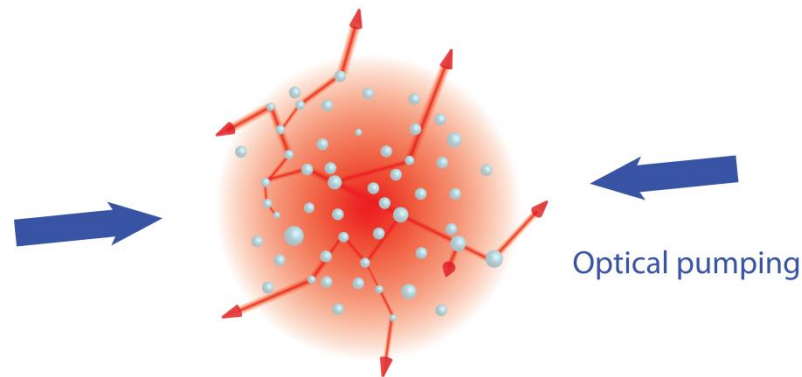
- Cavity Laser



Ingredients:

- Gain Medium
- Cavity
→ Feedback & Mode Selection

- Random Laser



- Gain Medium
- **Multiple scattering**

V.S. Letokhov, Sov. Phys. JETP 26, 835-840 (1968)

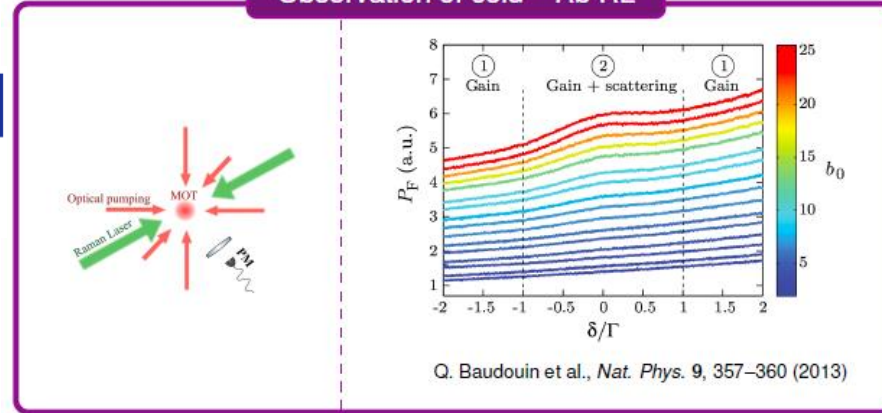


1939–2009

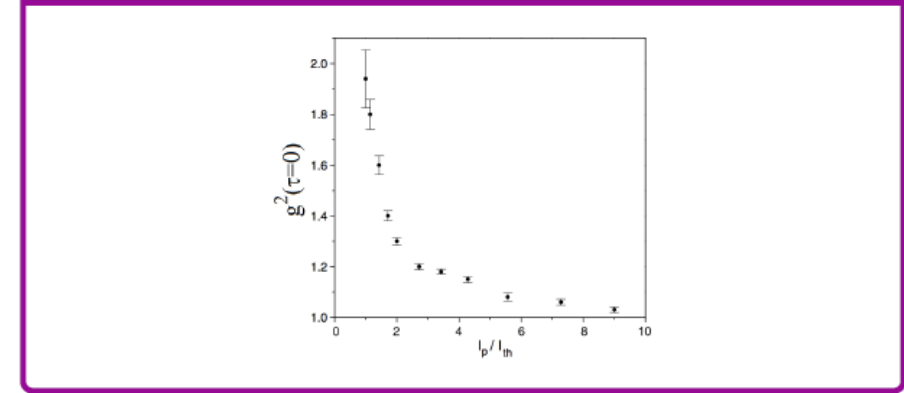
Atomic physics laboratory experiments

Goal : find spectroscopic signatures of gaseous **random lasing**

Observation of cold ⁸⁵Rb RL



H. Cao et al., *Phys. Rev. Lett.* 86, 4524 (2001)



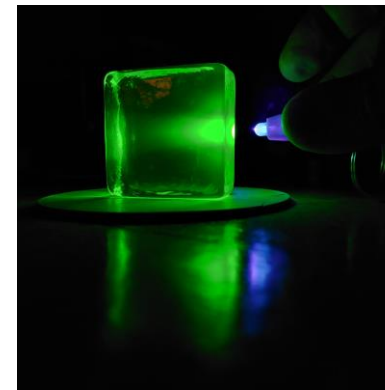
nature physics LETTERS
PUBLISHED ONLINE: 5 MAY 2013 | DOI:10.1038/NPHYS2614

A cold-atom random laser

Q. Baudouin, N. Mercadier[†], V. Guarrera[†], W. Guerin and R. Kaiser*

Intensity $g^{(2)}$ correlations in random fiber lasers: A random-matrix-theory approach

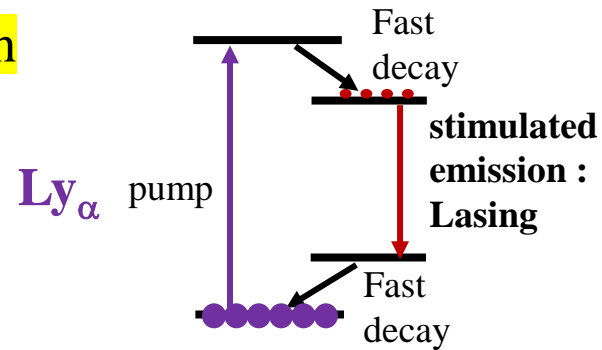
Ernesto P. Raposo, Iván R. R. González, Edwin D. Coronel, Antônio M. S. Macêdo, Leonardo de S. Menezes, Raman Kashyap, Anderson S. L. Gomes, and Robin Kaiser
Phys. Rev. A **105**, L031502 – Published 23 March 2022



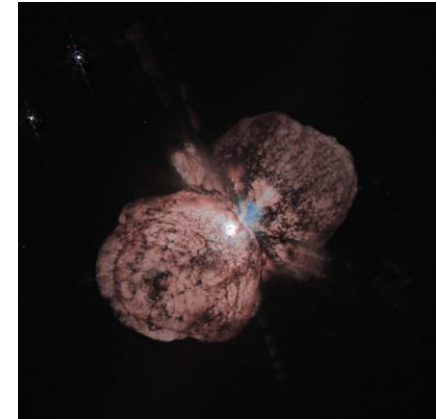
Bunching	$g^2(0)=2$
Superbunching	$g^2(0) > 2$
No bunching	$g^2(0)=1$?

Bonus : quantum astro-optics : coherent light sources

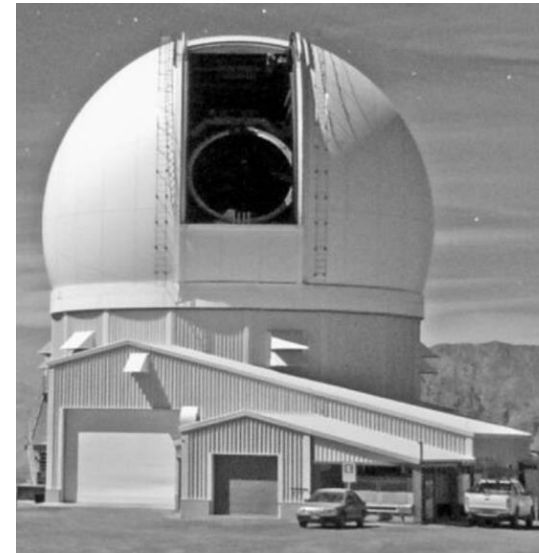
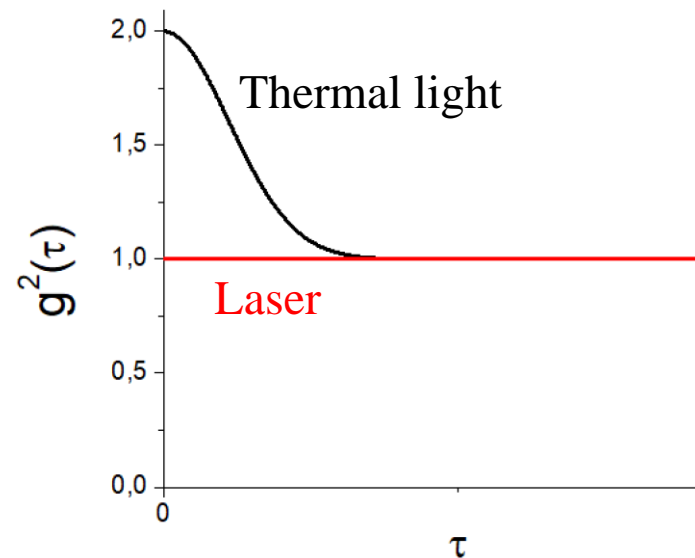
- Random laser with 4 level scheme



Eta Car
Fe II:
population inversion at
0.99 / 1.6 / 1.7 μm



- Lasing signature : $g^2(\tau)$ on a single telescope



SOAR
(Chile, southern hemisphere)

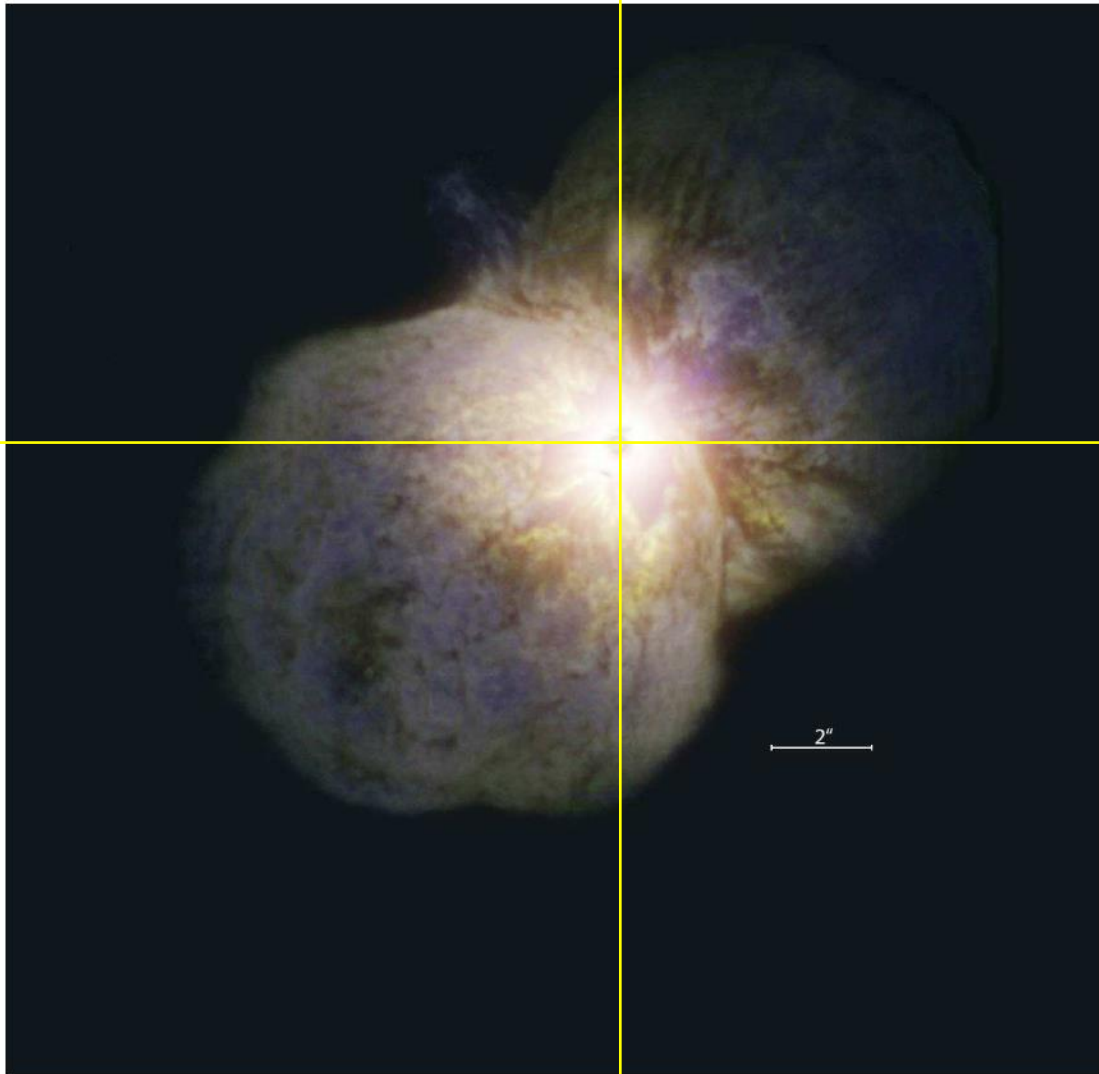


Fig. 2a.— The combined $\text{Br}\gamma$, H_2 , $[\text{Fe II}]$ image without the continuum subtraction; $\text{Br}\gamma$ (red), H_2 (green), and $[\text{Fe II}]$ (blue). North is up and east is left.

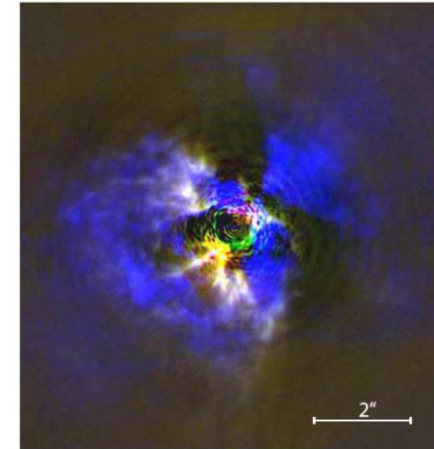


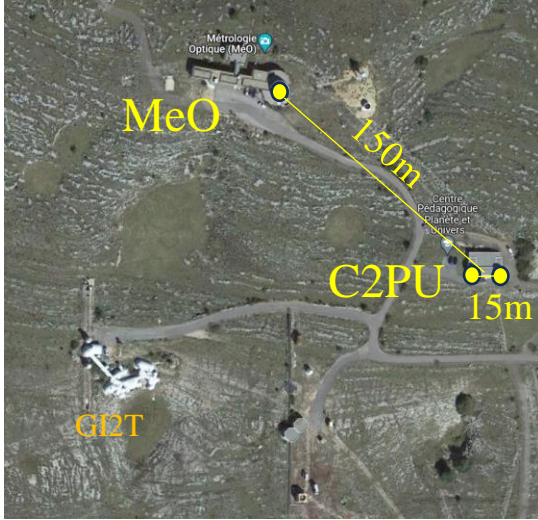
Fig. 2b.— The combined line - continuum image; $\text{Br}\gamma$ (red), H_2 (green), and $[\text{Fe II}]$ (blue). This figure shows the inner part of the Homunculus and region of the butterfly. Note the very different distribution of the $[\text{Fe II}]$ emission compared with $\text{Br}\gamma$ and H_2 . $\text{Br}\gamma$ and H_2 have nearly identical distributions, therefore their combined image appears white or yellowish.

Benchmarking @ Calern

- WP2.1 : $g^2(r)$

yellow hypergiant : γ Cas : M4.5, 2.4 m''

O-type star : 10Lac : M4.88 0.11 m''



THE ASTROPHYSICAL JOURNAL, 869:37 (13pp), 2018 December 10
 © 2018. The American Astronomical Society. All rights reserved. <https://doi.org/10.3847/1538-4357/aaec04>

Angular Sizes and Effective Temperatures of O-type Stars from Optical Interferometry with the CHARA Array

Kathryn D. Gordon¹, Douglas R. Gies¹, Gail H. Schaefer², Daniel Huber³, Michael Ireland⁴, and D. John Hillier⁵
¹Center for High Angular Resolution Astronomy and Department of Physics and Astronomy, Georgia State University, P. O. Box 5060, Atlanta, GA 30302-5060, USA; kgordon@astro.gsu.edu
²The CHARA Array of Georgia State University, Mount Wilson Observatory, Mount Wilson, CA 91023, USA
³Institute for Astronomy, University of Hawaii'i, 2680 Woodlawn Drive, Honolulu, HI 96822, USA
⁴Research School of Astronomy & Astrophysics, Australian National University, Canberra, ACT 2611, Australia
⁵Department of Physics and Astronomy and Pittsburgh Particle Physics, Astrophysics, and Cosmology Center (PITT PACC), University of Pittsburgh, Pittsburgh, PA 15260, USA
 Received 2018 August 20; revised 2018 October 22; accepted 2018 October 22; published 2018 December 10

Identifier	Star Name	HD Number	Spectral Classification	V (mag)	B - V (mag)	V - K (mag)	T _{eff} (kK)	θ_{UD} (mas)
a	ζ Per	24912	O7.5 III(n)(f)	4.06	0.02	0.11	34.3 ± 0.8	0.216 ± 0.016
b	α Cam	30614	O9 Ia	4.29	0.05	0.05	29.4 ± 1.0	0.250 ± 0.014
c	λ Ori A	36861	O8 III(f)	3.47	0.01	-0.56	34.5 ± 0.8	0.219 ± 0.015
d	ζ Ori A	37742	O9.2 Ib	1.88	-0.11	-0.44	29.5 ± 1.0	0.546 ± 0.029
e	ζ Oph	149757	O9.2 IVnn	2.56	0.02	-0.06	32.1 ± 1.3	0.532 ± 0.010
f	10 Lac	214680	O9 V	4.88	-0.21	-0.62	35.5 ± 0.5	0.11 ± 0.02

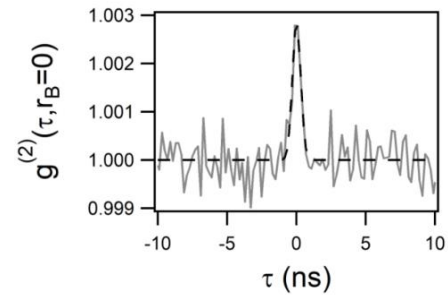
- WP3.1 : $g^2(\tau)$

P-Cygni : M4.82
 (η -Car of the north)

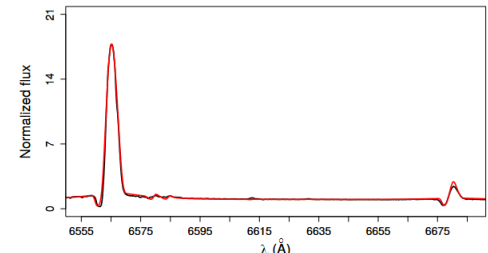
Combined spectroscopy and intensity interferometry to determine the distances of the blue supergiants P Cygni and Rigel FREE

E S G de Almeida ✉, M Hugbart ✉, A Domiciano de Souza, J-P Rivet, F Vakili, A Siciak, G Labeyrie, O Garde, N Matthews, O Lai, D Vernet, R Kaiser, W Guerin
[Author Notes](#)

Monthly Notices of the Royal Astronomical Society, Volume 515, Issue 1, September 2022, Pages 1–12, <https://doi.org/10.1093/mnras/stac1617>



H α $\lambda=656.3$ nm



Looking for further targets

A **B[e] star**, frequently called a **B[e]-type star**, is a **B-type star** with distinctive **forbidden** neutral or low ionisation **emission lines** in its spectrum. The designation results from combining the spectral class **B**, the lowercase **e** denoting emission in the spectral classification system, and the surrounding square brackets signifying forbidden lines. These stars frequently also show strong hydrogen emission lines, but this feature is present in a variety of other stars and is not sufficient to classify a B[e] object. Other observational characteristics include optical **linear polarization** and often **infrared** radiation that is much stronger than in ordinary B-class stars, called **infrared excess**. As the B[e] nature is transient, B[e]-type stars might exhibit a normal B-type spectrum at times, and hitherto normal B-type stars may become B[e]-type stars.



Nebulosity around the B[e] star HD 87643

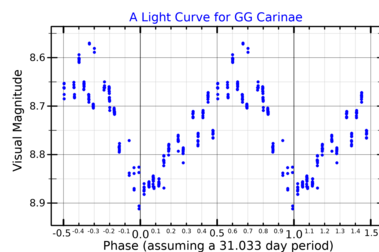
Discovery [\[edit\]](#)

Many **Be stars** were discovered to have spectral peculiarities. One of these peculiarities was the presence of **forbidden spectral lines** of ionised iron and occasionally other elements.^[1]

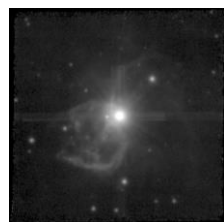
In 1973 a study of one of these stars, **HD 45677** or **FS CMA**, showed an **infrared excess** as well as forbidden lines of **[O I]**, **[S II]**, **[Fe II]**, **[Ni II]**, and many more.^[2]

In 1976 a study of **Be stars** with **infrared excesses** identified a subset of stars which showed forbidden emission lines from ionised iron and some other elements. These stars were all considered to be distinct from the classical main sequence **Be stars**, although they appeared to consist of a wide range of different types of star. The term **B[e] star** was coined to group these stars.^[3]

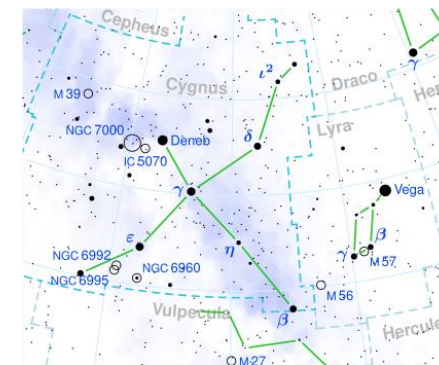
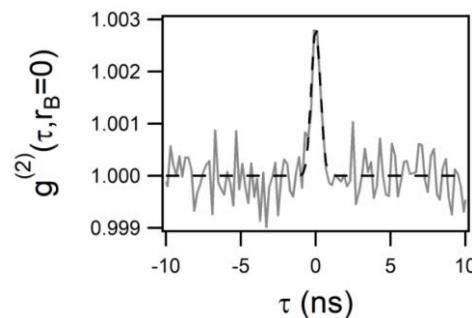
GG Car (V=8.70) -> ~ 2.4 kpc



HR Car (V=8) -> ~4.8 kpc



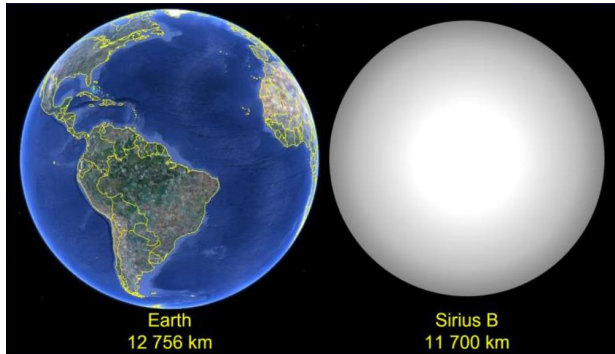
P-Cygni (V=4.82) -> ~ 1.55 kpc



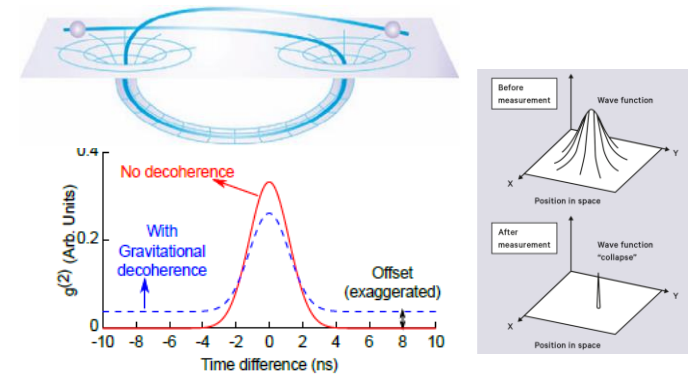
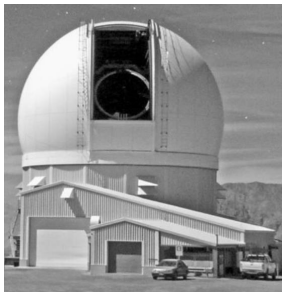
$\lambda=656.3 \text{ nm}$

Beyond IC4Stars

- **Ultra-high angular resolution in astrophysics : $g^2(\mathbf{r})$**



- **Quantum eye on astrophysics : $g^2(\tau)$**



New J. Phys. 20, 063016 (2018)

Space QUEST mission proposal: experimentally testing decoherence due to gravity

Siddarth Koduru Joshi^{1,2} , Jacques Pienaar¹ , Timothy C Ralph³, Luigi Cacciapuoti⁴, Will McCutcheon², John Rarity², Dirk Gigenbach⁵, Jin Gyu Lim⁶ , Vadim Makarov⁷, Ivette Fuentes¹

[Show full author list](#)

Published 12 June 2018 • © 2018 The Author(s). Published by IOP Publishing Ltd on behalf of Deutsche Physikalische Gesellschaft

[New Journal of Physics, Volume 20, June 2018](#)

Citation Siddarth Koduru Joshi *et al* 2018 *New J. Phys.* **20** 063016

DOI 10.1088/1367-2630/aac58b

Science

Current Issue First release papers Archive About

HOME > SCIENCE > VOL. 366, NO. 6461 > SATELLITE TESTING OF A GRAVITATIONALLY INDUCED QUANTUM DECOHERENCE MODEL

REPORT

f X in

Satellite testing of a gravitationally induced quantum decoherence model

PING XU , YIQIU MA , JI-GANG REN , HAI-LIN YONG , TIMOTHY C. RALPH, SHENG-KAI LIAO , JUAN YIN , WEI-YUE LIU , WEN-QI CAI, [...], AND

JIAN-WEI PAN  +13 authors [Authors Info & Affiliations](#)

SCIENCE • 19 Sep 2019 • Vol 366, Issue 6461 • pp. 132-135 • DOI: 10.1126/science.aay5820

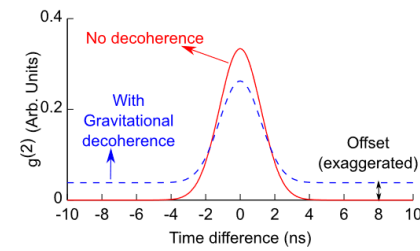
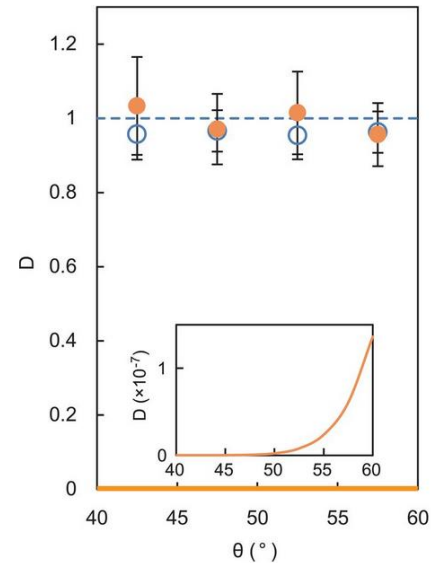


Figure 3. Illustration of the gravitational decoherence effect. Consider a temporal cross correlation histogram $g^{(2)}$ between the arrival times of photons at the OGS and on the ISS. The area of the peak represents the number of photon pairs while the number of singles events is obtained from the photon counting module. The gravitational decoherence effect from [1], should result in a decrease in the number of photon pairs (area) without altering the singles rate, the position of or the width of the peak. This is depicted in the above figure where the red (solid) curve shows the $g^{(2)}$ in the absence of a gravitational field gradient (i.e., without gravitational decoherence effect) and the blue (dashed) curve shows the effect of gravitational decoherence between an OGS and the ISS at the zenith 400 km away using a source of time entangled photon pairs with a coherence time of 0.8 ps. The offset shown here is grossly exaggerated and for illustrative purposes only. Therefore, to observe the gravitational decoherence effect we cannot rely on measuring the change in noise/background accidental count rates, instead we rely on measuring the change in area between the two curves. We emphasize that the gravitational decoherence effect can still be observed despite a detector jitter of several ns. Reducing the jitter only improves the signal to noise ratio (SNR) by reducing the accidental coincidence rate (which contributes to the offset).



Inset: magnified view of the predictions of event formalism.

both spacetime settings are plotted in **Fig. 4, A and B (26)**, respectively. Given our experimental condition with $d_t \sim 0.07$ mm (≈ 0.2 ps) (26) and satellite altitude of ~ 500 km, event formalism predicts decorrelation effects, $D(\theta) < 10^{-6}$ for $40^\circ < \theta < 60^\circ$ (smooth



Thank you for your attention

Open positions (PhD, postdoc)